



ORIGINAL ARTICLE

Rapid loss of group 1 innate lymphoid cells during blood stage *Plasmodium* infection[†]

Susanna S Ng^{1,2} , Fernando Souza-Fonseca-Guimaraes^{3,4}, Fabian de Labastida Rivera¹, Fiona H Amante¹, Rajiv Kumar^{1,5} , Yulong Gao^{6,7}, Meru Sheel⁸, Lynette Beattie¹, Marcela Montes de Oca¹, Camille Guillerey⁶, Chelsea L Edwards^{1,7}, Rebecca J Faleiro¹, Teija Frame¹, Patrick T Bunn¹, Eric Vivier^{9,10}, Dale I Godfrey^{11,12}, Daniel G Pellicci^{11,12}, J Alejandro Lopez², Katherine T Andrews², Nicholas D Huntington^{4,13}, Mark J Smyth⁶, James McCarthy^{14*} & Christian R Engwerda^{1*}

¹Immunology and Infection Laboratory, QIMR Berghofer Medical Research Institute, Herston, QLD, Australia

²School of Natural Sciences, Griffith University, Nathan, QLD, Australia

³Faculty of Medicine, Dentistry and Health Sciences, University of Melbourne, Melbourne, VIC, Australia

⁴Molecular Immunology Division, The Walter and Eliza Hall Institute of Medical Research, Parkville, VIC, Australia

⁵Department of Biochemistry, Banaras Hindu University, Varanasi, India

⁶Immunology in Cancer and Infection, QIMR Berghofer Medical Research Institute, Herston, QLD, Australia

⁷School of Medicine, University of Queensland, Herston, QLD, Australia

⁸National Centre for Immunisation Research and Surveillance, Westmead, NSW, Australia

⁹Aix Marseille Université, CNRS, INSERM, CIML, Marseille, France

¹⁰Service d'Immunologie, APHM, Hôpital de la Conception, Marseille, France

¹¹Department of Microbiology and Immunology, Peter Doherty Institute for Infection and Immunity, University of Melbourne, Melbourne, VIC, Australia

¹²Australian Research Council Centre of Excellence for Advanced Molecular Imaging, University of Melbourne, Melbourne, VIC, Australia

¹³Department of Medical Biology, The University of Melbourne, Melbourne, VIC, Australia

¹⁴Clinical Tropical Medicine, QIMR Berghofer Medical Research Institute, Herston, QLD, Australia

Correspondence

Christian R. Engwerda, Immunology and Infection Laboratory, QIMR Berghofer Medical Research Institute, Herston, QLD, Australia.

E-mail: Christian.Engwerda@qimr.edu.au

Received 21 August 2017;

Revised 9 November 2017

and 4 December 2017;

Accepted 5 December 2017

doi: 10.1002/cti.1003

Clinical & Translational Immunology
2018; 7: e1003

*These authors contributed equally to the work.

†This work was made possible through Queensland State Government funding. The research was supported by grants and fellowships from the National Health and

Abstract

Objectives. Innate lymphoid cells (ILCs) share many characteristics with CD4⁺ T cells, and group 1 ILCs share a requirement for T-bet and the ability to produce IFN γ with T helper 1 (Th1) cells. Given this similarity, and the importance of Th1 cells for protection against intracellular protozoan parasites, we aimed to characterise the role of group 1 ILCs during *Plasmodium* infection. **Methods.** We quantified group 1 ILCs in peripheral blood collected from subjects infected with *Plasmodium falciparum* 3D7 as part of a controlled human malaria infection study, and in the liver and spleens of *PcAS*-infected mice. We used genetically-modified mouse models, as well as cell-depletion methods in mice to characterise the role of group 1 ILCs during *PcAS* infection. **Results.** In a controlled human malaria infection study, we found that the frequencies of circulating ILC1s and NK cells decreased as infection progressed but recovered after volunteers were treated with antiparasitic drug. A similar observation was made for liver and splenic ILC1s in *P. chabaudi chabaudi* AS (*PcAS*)-infected mice. The decrease in mouse liver ILC1 frequencies was associated with increased apoptosis. We also identified a population of cells

Medical Research Council of Australia (NHMRC) and Australia Research Council (ARC), as well as Australian Postgraduate Awards through Griffith University, School of Natural Sciences and the University of Queensland, School of Medicine and an INSPIRE Fellowship to Rajiv Kumar provided by the Indian government Department of Science and Technology. Funding for the CHMI studies was provided by Medicines for Malaria Venture (MMV) from grants awarded by the Wellcome Trust and Bill and Melinda Gates Foundation

within the liver and spleen that expressed both ILC1 and NK cell markers, indicative of plasticity between these two cell lineages. Studies using genetic and cell-depletion approaches indicated that group 1 ILCs have a limited role in antiparasitic immunity during *PcAS* infection in mice. **Discussion.** Our results are consistent with a previous study indicating a limited role for natural killer (NK) cells during *Plasmodium chabaudi* infection in mice. Additionally, a recent study reported the redundancy of ILCs in humans with competent B and T cells. Nonetheless, our results do not rule out a role for group 1 ILCs in human malaria in endemic settings given that blood stage infection was initiated intravenously in our experimental models, and thus bypassed the liver stage of infection, which may influence the immune response during the blood stage. **Conclusion.** Our results show that ILC1s are lost early during mouse and human malaria, and this observation may help to explain the limited role for these cells in controlling blood stage infection.

Keywords: inflammation, natural killer cells, parasitic–protozoan.

INTRODUCTION

Innate lymphoid cells (ILCs) resemble T helper (Th) cells in terms of their characteristic transcription factors and functions.¹ Groups 1, 2 and 3 ILCs make up the ILC repertoire, and these groups are similar to Th1, Th2 and Th17 cells, respectively. In contrast to Th cells of the adaptive immune system, ILCs do not express antigen-specific T-cell receptors.² ILCs have both protective and pathogenic roles in infectious and inflammatory diseases.^{3,4} However, a recent study has suggested that ILCs are redundant in the presence of a competent B and T-cell response in humans.⁵

Group 1 ILCs consist of conventional natural killer (cNK) cells and ILC1s.^{1,6} These cell subsets share common developmental requirements for the transcription factor T-bet and their ability to produce the pro-inflammatory cytokine IFN γ .⁶ However, the relationship between these cells is still widely debated. Liver ILC1s are a specialised subset of group 1 ILCs also known as tissue-resident NK (trNK) cells.⁷ Other ILC1s have also been identified in the uterus,⁸ spleen,⁹ salivary gland,¹⁰ kidney,¹¹ adipose tissue¹² and gastrointestinal tract.⁹ These different tissue-resident subsets have unique cell surface phenotypes and functions.^{4,9,13}

Malaria is a globally important infectious disease caused by protozoan parasites belonging to the genus *Plasmodium*. Following infection, a Th1-dependent immune response can develop in the

mammalian host, aiding clearance of parasites via IFN γ -dependent mechanisms.^{14,15} IFN γ production by antigen-specific CD4⁺ T cells during *P. chabaudi* AS (*PcAS*) infection in mice has been reported,¹⁶ and increased parasite growth was observed following IFN γ neutralisation.¹⁷ The relationship between IFN γ production and control of parasite growth has also been reported in humans during blood stage *Plasmodium falciparum* (*Pf*) infection.¹⁸ Additionally, we recently showed an inverse correlation between IFN γ levels and parasite burden during controlled human malaria infection (CHMI) with *Pf*.¹⁹ However, the secretion of IFN γ contributes to an inflammatory environment that can also contribute to pathology.^{18,20–24} While the adaptive immune response generated in response to *Plasmodium* infection has been well characterised, less is known about the innate immune response following infection. Early studies revealed that the depletion of NK cells with anti-asialo GM1 antibody resulted in increased parasitaemia during *PcAS* infection.²⁵ However, the effects of this treatment on dendritic cell (DC) function²⁶ and the depletion of other cell subsets, such as basophils,²⁷ may impact the interpretation of these results. In fact, depletion of NK cells in mice via administration of anti-NK1.1 antibody resulted in no effect on the course of *P. chabaudi adami* 556KA infection.²⁸ However, evidence for direct interactions between human NK cells and *Pf*

parasitised red blood cells (pRBC) *in vitro*, which stimulates production of IFN γ , has been reported.²⁹

Given that group 1 ILCs function like Th1 cells, and little is known about their roles during *Plasmodium* infection, we examined these cells, as well as the more well-studied innate-like T cells (including $\gamma\delta$ T cells,²⁸ invariant natural killer T (iNKT) cells^{30,31} and mucosal-associated invariant T (MAIT) cells³²) in volunteers infected with *Pf* in CHMI studies. Concurrently, we also investigated the role of ILC1s in C57BL/6J mice infected with *PcAS*, which causes a chronic, nonlethal infection.³³ We report that cNK cells and ILC1s had a limited role in controlling peripheral blood parasitaemia in mice infected with *PcAS*. However, we found a loss in circulating NK cells and ILC1s in volunteers participating in CHMI studies with *Pf*, which was independent of parasite burden. A similar loss of ILC1s was also observed in the liver and spleen of mice infected with *PcAS*. Furthermore, we report a novel NK1.1⁺ NKp46⁺ population that expressed both the ILC1 marker CD49a and the cNK marker DX5 (CD49b) in the livers of *PcAS*-infected mice, suggesting plasticity between these cell populations.

RESULTS

The frequency and number of ILC1s declined during blood stage *Pf* infection

NK and $\gamma\delta$ T cells produce IFN γ in response to *Pf* infection.^{34–36} To gain a better understanding of IFN γ production by innate immune cells, including more recently identified ILC1s and innate-like T cells, we examined these cell populations during an experimentally induced blood stage malaria infection in healthy volunteers with no prior exposure to malaria or residence in malaria-endemic regions.^{37,38} Human PBMCs were isolated from blood drawn prior to infection (day 0) and at 7 days postinfection (p.i.), prior to drug treatment (Figure 1a). We then identified group 1 ILCs (CD56⁻ CD127⁺ T-bet⁺ ILC1s and NK cells), group 1 ILC-like cells (CD56⁺ CD127⁺ T-bet⁺) (Figure 1b and Supplementary figure 1A), as well as innate-like T cells ($\gamma\delta$ T cells [CD3⁺, $\gamma\delta$ TCR⁺], iNKT cells [CD3⁺, CD1d PBS44 tetramer⁺] and MAIT cells [CD3⁺, CD8⁺, CD161⁺, TCR V α 7.2⁺]) (Supplementary figure 1B).

We found the frequency and number of NK cells, CD56⁺ CD127⁺ ILC1s and $\gamma\delta$ T cells were reduced at 7 days p.i., compared to day 0 (Figures 1d and e). NK cells and all innate-like T-

cell populations produced IFN γ upon PMA + ionomycin restimulation; however, only the frequency of IFN γ ⁺ iNKT, $\gamma\delta$ T and MAIT cells was significantly reduced at day 7, compared to day 0 (Figure 1f). The white blood cell count (WBC) in volunteers was not significantly different between days 0 and 7 p.i. (Figure 1c), indicating that a general loss of blood leukocytes during infection did not account for these results. When the frequency and numbers of these cells were examined in one cohort after volunteers were treated with antiparasitic drug, we found they had recovered and in some cases were increased, relative to pre-infection levels (Table 1).

Parasite accumulation in volunteers, as measured by the area under the curve (AUC) of blood parasitaemia curves (Figure 1a), was plotted against the frequency or cell number of each cell subset shown in Figure 1 at day 7 p.i. to identify any relationships with parasite burden. However, no significant relationships were found for any ILC or innate-like T cells ($P > 0.05$ for all cell subsets; data not shown). Similar results were obtained when the parasite multiplication rate (PMR) over time in each volunteer was plotted against corresponding ILC or innate-like T-cell frequencies or cell number. Together, these results show the frequency and cell number of group 1 ILCs were reduced following first exposure to blood stage *Pf* but this reduction was independent of parasite burden or PMR and recovered following antiparasitic drug treatment. These data suggest that NK cells and ILC1s either have increased cell death, decreased cell proliferation or sequester to tissues following *Pf* infection.

A loss of liver trNK cells and splenic ILC1s during *PcAS* infection

To further investigate ILCs in tissues during malaria, we next employed a mouse model of *PcAS* infection. A novel subset of liver ILC1s (trNK cells) has been reported in mice and humans.^{7,39} We examined these cells, as well as splenic ILC1s,⁹ because of the importance of the liver and spleen as blood filtering organs during *Plasmodium* infection.^{40,41} We identified liver ILC1s that were lineage (Lin⁻; CD3, CD5, CD19)-negative, CD45⁺ NK1.1⁺ NKp46⁺ CD49a⁺ DX5⁻ (Figure 2a). These were distinct from splenic ILC1s, identified as Lin⁻ CD45⁺ NK1.1⁺ NKp46⁺ Eomes⁻ CD127⁺ (Figure 2b). We found a decrease in the frequency and number of liver (Figure 2c) and spleen ILC1s

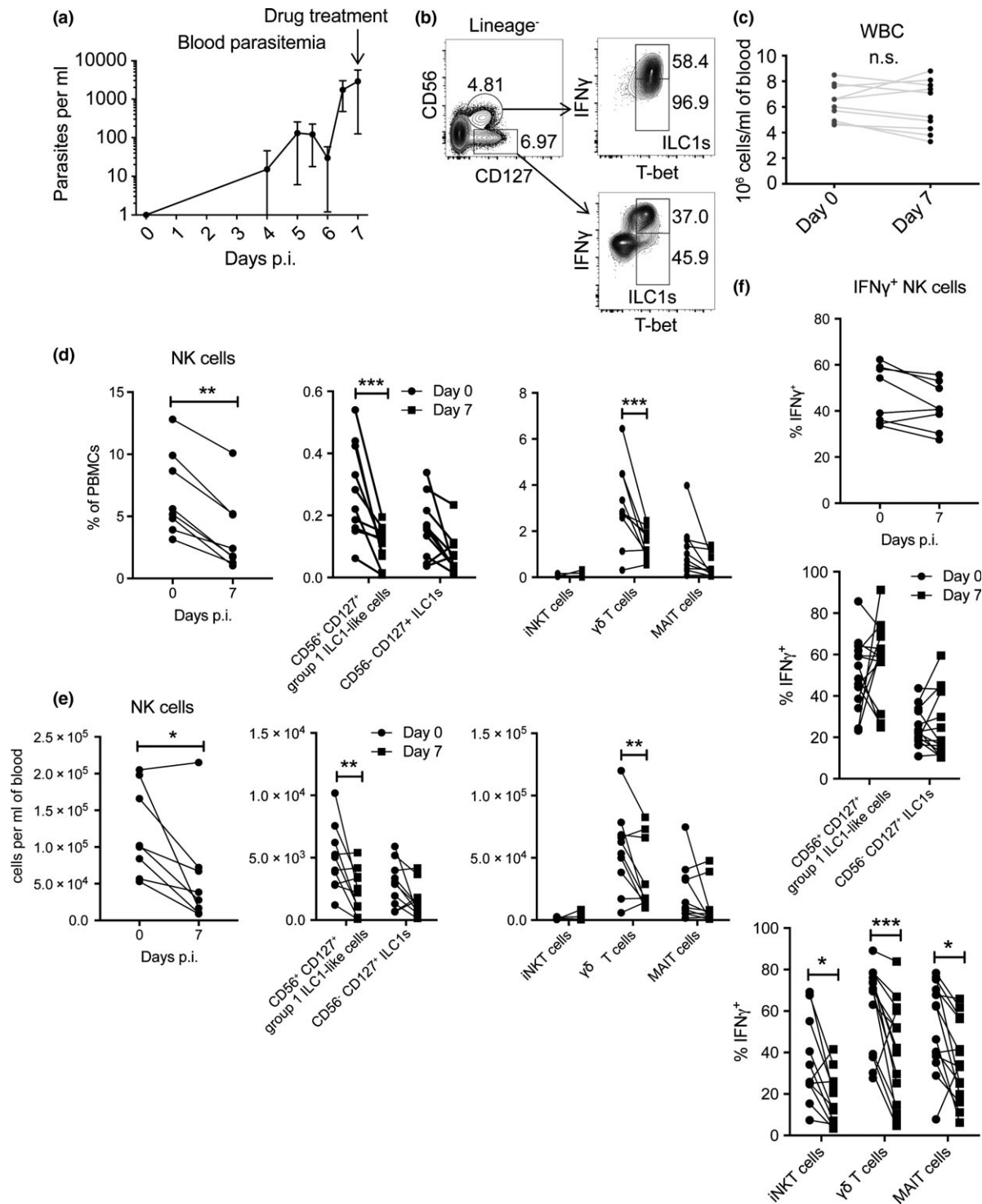


Figure 1. ILC and innate-like T-cell frequencies decrease following *P. falciparum* infection. Representative blood parasitaemia curve over the first 7 days of infection from a single cohort ($n = 6$) (a). Group 1 ILC and group 1 ILC-like subsets were identified by flow cytometry as indicated in the gating strategy (b). White blood cell counts for each patient at days 0 and 7 are depicted (c). The frequencies (d) and cell numbers (e) of group 1 ILC, group 1 ILC-like and innate-like T-cell subsets are shown. The proportion of each subset producing IFN γ is shown (f). The data from b–f represent results from one to three cohorts ($n = 8–14$). Error bars represent the mean \pm standard deviation (SD) (a). Comparisons between days 0 and 7 were made using the Wilcoxon (paired, nonparametric) test for NK cells and a two-way ANOVA with Sidak’s multiple comparisons test for other subsets. * $P < 0.05$, ** $P < 0.01$, *** $P < 0.001$.

Table 1. Frequencies and total cell numbers of innate lymphoid cells and innate-like T cells

Cell population	% of PBMCs		Cell number	
	Naive	D14	Naive	D14
CD56 ⁻ CD127 ⁺ ILC1s	0.201 ± 0.043 ^a	7.657 ± 1.473*	3458 ± 803	113 068 ± 21 815*
CD56 ⁺ CD127 ⁺ ILC1s	0.351 ± 0.060	0.497 ± 0.100	5955 ± 1084	7699 ± 1786
ILC2s	0.005 ± 0.001	0.024 ± 0.006*	88 ± 20	348 ± 83*
ILC3s	0.075 ± 0.012	0.147 ± 0.019*	1311 ± 263	2226 ± 326
NK cells	8.555 ± 1.922	10.073 ± 3.126	144 535 ± 29 365	144 678 ± 44 178
iNKT cells	0.071 ± 0.019	0.040 ± 0.006	1262 ± 374	587 ± 88*
γδ T cells	3.042 ± 0.629	4.957 ± 0.898*	50 915 ± 10 533	77 968 ± 14 438*
MAIT cells	1.245 ± 0.578	1.514 ± 0.747	22 785 ± 11 294	23 625 ± 11 166
IFNγ ⁺ CD56 ⁻ CD127 ⁺ ILC1s	0.147 ± 0.037	0.374 ± 0.069*	2521 ± 640	5670 ± 1142
IFNγ ⁺ CD56 ⁺ CD127 ⁺ ILC1s	0.162 ± 0.038	0.390 ± 0.095	2762 ± 592	6024 ± 1661
IL-13 ⁺ ILC2s	0.002 ± 0.001	0.004 ± 0.001	42 ± 14	59 ± 13
IL-22 ⁺ ILC3s	0.007 ± 0.002	0.017 ± 0.005	103 ± 22	238 ± 53
IFNγ ⁺ NK cells	3.670 ± 1.041	4.763 ± 1.585	61 618 ± 16 064	67 648 ± 22 301
IFNγ ⁺ iNKT cells	0.017 ± 0.005	0.008 ± 0.001	313 ± 119	124 ± 17
IFNγ ⁺ γδ T cells	1.664 ± 0.413	3.338 ± 0.667*	28 636 ± 7363	52 038 ± 10 180*
IFNγ ⁺ MAIT cells	0.643 ± 0.379	0.684 ± 0.309	12 025 ± 7268	10 625 ± 4641

^aMean ± standard error of mean (SEM) of $n = 6$ from one cohort treated with artefenomel (OZ439) on day 7 (D7) post-infection.

* P value < 0.05.

Comparisons between days 0 (naive) and 14 (D14) were made using the Wilcoxon (paired, nonparametric) test.

(Figure 2d) 5 days p.i. with *PcAS*, although statistical differences were only reached in cell frequencies (Figures 2c and d). In contrast, liver cNK cells (NK1.1⁺ NKp46⁺ CD49a⁻ DX5⁺) increased in cell number over this same time period (Figure 2e).

ILC1s exhibit a more apoptotic phenotype than cNK cells

One possible explanation for the reduced ILC1 frequency and number following *PcAS* infection could be increased apoptosis. To test this, we stained liver ILC1s *ex vivo* to assess Caspase-3/7 expression as a marker of apoptosis from days 1 to 4 p.i. (Figure 3a). Flow cytometry analysis revealed approximately 20% of liver ILC1s expressing Caspase-3/7 in naive C57BL/6 mice (Figure 3b). Following *PcAS* infection, the frequency of Caspase-3/7-expressing ILC1s increased further at 2 days p.i., compared to naive cells. Therefore, increased apoptosis may at least partly explain the reduced liver ILC1 frequency early after *PcAS* infection.

Emergence of a CD49a⁺ DX5⁺ double-positive population

We also identified a population of cells within the liver and spleen that were Lin⁻ CD45⁺ NK1.1⁺ NKp46⁺ CD49a⁺ DX5⁺ (herein referred to as the

CD49a⁺ DX5⁺ double-positive' population) (Figures 4a and b). This population was readily detected 5 days p.i. and increased as infection progressed (Figure 4c). This CD49a⁺ DX5⁺ double-positive population was detected at lower frequencies at 28 days p.i. when the ratio of ILC1s to cNK cells resembled that of naive samples, although full recovery of ILC1 number or frequency was not evident at this time point (Figure 4c). Interestingly, the CD49a⁺ DX5⁺ double-positive population expressed the cNK cell marker CD62L and the ILC1 marker TNF-related apoptosis-inducing ligand (TRAIL) at intermediate levels (Figure 4d), suggesting they may represent a transitional population between cNK cells and ILC1s.

Systemic cNK cell and ILC1 depletion do not affect blood parasitaemia

We next investigated the role of ILC1s during *Plasmodium* infection, given their transcriptional and functional resemblance to Th1 cells,^{1,6} and previous reports indicating important roles for NK cells during *PcAS* infection.²⁵ WT, *Rag1*^{-/-} and *Rag2*^{-/-}γ_c^{-/-} mice were infected with *PcAS*, which caused a nonlethal, chronic infection in control WT mice.³³ Unexpectedly, immunodeficient *Rag2*^{-/-}γ_c^{-/-} mice (deficient in all lymphocytes) had a delayed peak parasitaemia, compared to *Rag1*^{-/-}

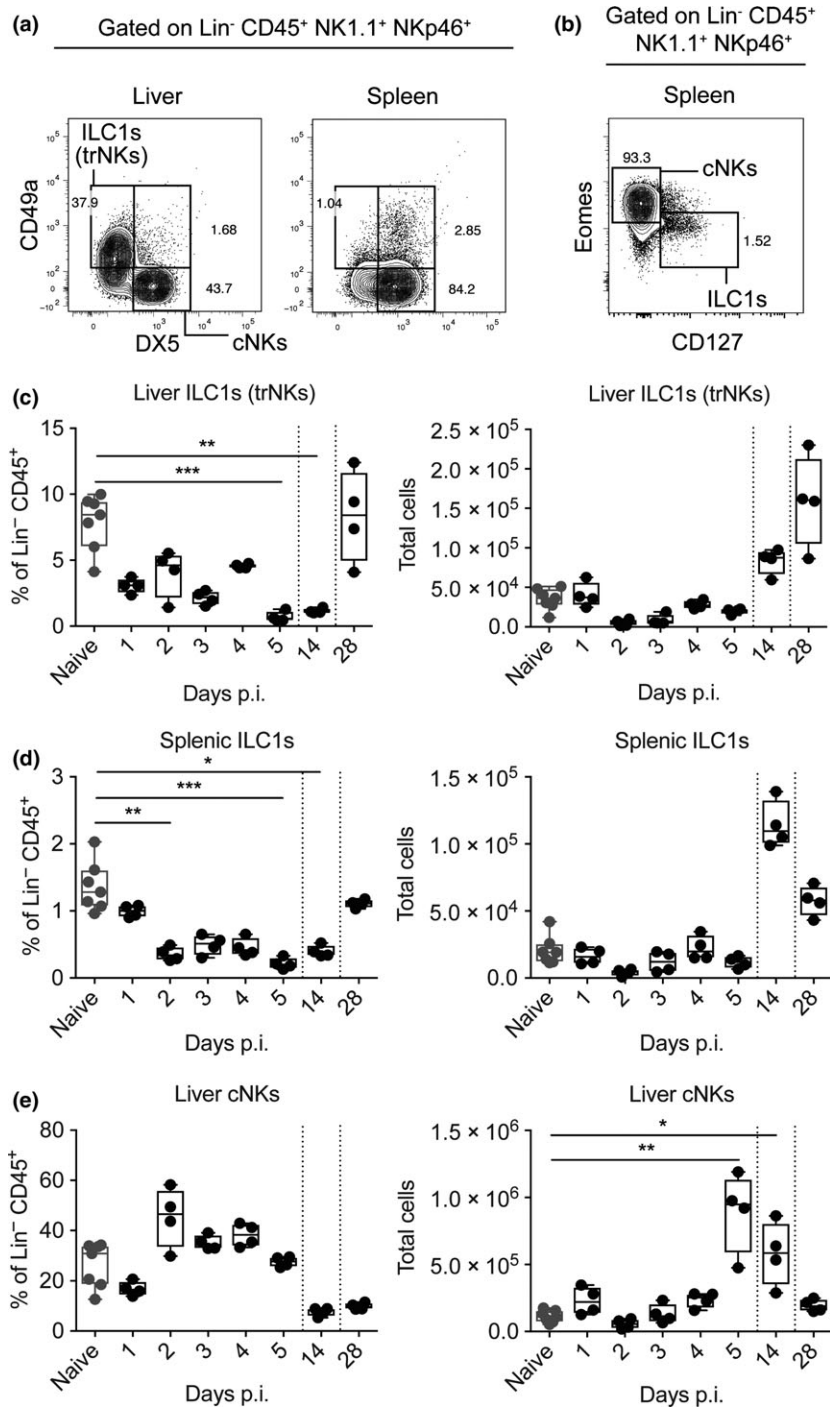


Figure 2. ILC1s decrease in number and frequency 5 days postinfection with *PcAS*. The gating strategy to identify liver ILC1s, a population that is absent in the spleen is shown (a), as well as a summary of the gating strategy for splenic ILC1s (b). These are representative plots from naïve animals. Liver and spleen single-cell suspensions in naïve and *PcAS*-infected mice were stained to determine ILC1 frequencies and cell numbers at days 1–5, 14 and 28 postinfection. Liver ILC1 (c), splenic ILC1 (d) and liver cNK (e) frequencies and absolute numbers are shown. Data are representative of two experiments from cohorts of at least $n = 4$ mice per time point. Comparisons were made using the Kruskal–Wallis test accompanied by the Dunn’s multiple comparisons test. * $P < 0.05$, ** $P < 0.01$.

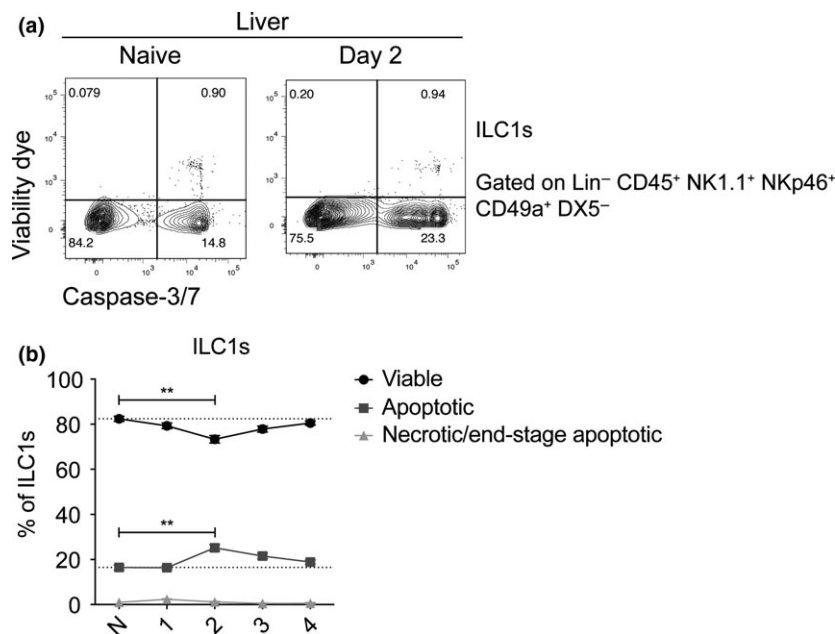


Figure 3. Liver ILC1s exhibit a more apoptotic phenotype than cNK cells. Liver single-cell suspensions were stained for a viability marker, ILC1 surface markers, followed by staining for Caspase-3/7. The representative plots from naïve and day 2 p.i. are shown **(a)** where viability dye⁺ Caspase-3/7⁻ = dead cells, viability dye⁺ Caspase-3/7⁺ = necrotic cells, **(b)** viability dye⁻ Caspase-3/7⁺ = apoptotic cells, and viability dye⁻ Caspase-3/7⁻ = live cells. The relative frequencies of viable, apoptotic and necrotic/end-stage apoptotic ILC1s are shown. Data represent mean ± SEM from one experiment where $n = 3$ for naïve mice and $n = 4$ for *PcAS*-infected mice. Comparisons were made using the Kruskal–Wallis test accompanied by the Dunn’s multiple comparisons test. ** $P < 0.01$.

mice that were only deficient in B and T cells (Figure 5a). To determine whether the delayed peak parasitaemia observed in *Rag2*^{-/-} γ_c ^{-/-} mice could be attributed to the absence of cNKs, we infected *Ncr1-iCre x Mcl1^{fl/fl}* mice with *PcAS*. Myeloid cell leukaemia sequence-1 (*Mcl1*) is critical for the maintenance of mature NK cells and ILC1s.⁴² Therefore, these cells were absent in mice lacking *Mcl1* gene expression in NKp46 (encoded by the *Ncr1* gene)-positive cells. Surprisingly, these mice were able to control parasite growth and had similar blood parasitaemia to *Ncr1-iCre*^{+/-} control mice (Figure 5b). Hence, the delay in peak parasitaemia in *Rag2*^{-/-} γ_c ^{-/-} mice, relative to *Rag1*^{-/-} mice, was not likely caused by the absence of NK cells or ILC1s but instead, possibly reflects changes in either the activity of phagocytic cells or alterations to parasite growth in the blood of *Rag2*^{-/-} γ_c ^{-/-} mice.

We next focused attention specifically on ILC1s by infecting *Ncr1-iCre x Tgfb2^{fl/fl}* mice with *PcAS*. These mice lack *Tgfb2* gene expression in NKp46-positive cells and have significantly reduced ILC1 numbers.⁶ Despite this, these mice were still able to control parasite growth as efficiently as control animals (Figure 5c). Given previous contradictory

reports on the role of cNK cells during malaria,^{25–29} we next confirmed the above results in 2 other cNK cell- and ILC1-deficient models. First, we treated mice with α -NK1.1 mAb (depletes cNK cell and ILC1s) and found no effect on the ability to control parasite growth, compared with control mice (Figure 5d). Second, we used diphtheria toxin (DT) to deplete cNK cells and ILC1s in *Ncr1-iCre x iDTR* mice and again found no change in the ability of mice to control infection, relative to control-treated animals (Figure 5e). Together, these data indicate limited roles for cNK cells and ILC1s in antiparasitic immunity during *PcAS* infection.

DISCUSSION

Here, we show a reduction in the frequency of circulating ILC1s, NK cells and innate-like T cells in healthy volunteers infected for the first time with *Pf*. This finding was akin to the decrease in frequencies and numbers of peripheral T cells during acute *Pf* malaria in Ghanaian children.⁴³ Similar observations were made for spleen and liver ILC1s in C57BL/6 mice infected with *PcAS*, accompanied by increased apoptosis in the latter cell population. Further studies on the roles of

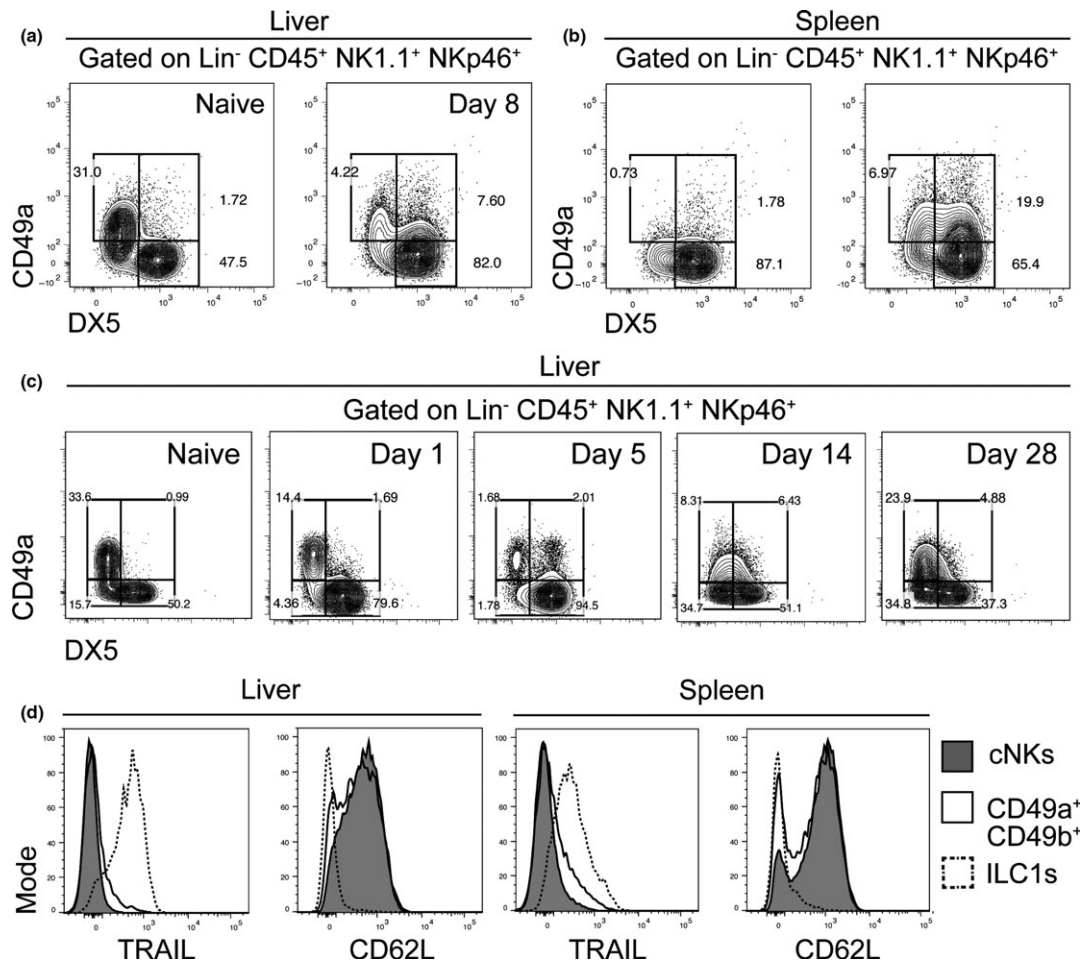


Figure 4. A novel CD49a⁺ DX5⁺ population emerges. Representative plots show a novel CD49a⁺ DX5⁺ double-positive population in the liver (a) and spleen (b) of infected mice. The double-positive population underwent changes during infection (c). Expression of TNF-related apoptosis-inducing ligand (TRAIL) and CD62L by the CD49a⁺ DX5⁺ double-positive population is shown (d). Data are representative of three experiments from cohorts of at least *n* = 4 mice.

ILC1s and NK cells during *PcAS* infection using cell depletion and genetically modified mice indicated a limited role for these cells in the control of blood parasitaemia. These results contrast earlier findings that reported NK cells confer protection during *Plasmodium* infection using anti-asialo GM1 to deplete NK cells,²⁵ but were consistent with more recent findings using anti-NK1.1 mAb for NK cell depletion.²⁸ Interestingly, a recent study in humans who had received a bone marrow transplant found that ILCs were redundant in the presence of competent B and T cells.⁵ Our data indicate this may also be the case in experimental malaria, but we cannot yet make definitive conclusions on the role of these cells in human malaria.

A recent study has reported that ILCs were irreversibly lost during acute HIV-1 infection.⁴⁴

Our findings in *PcAS*-infected mice indicate that liver and splenic ILC1s were lost in the first 5 days of infection but recovered as infection was controlled. Similarly, in volunteers participating in CHMI studies, the frequency and number of circulating ILC1s, NK cells and innate-like T cells all fell in the first 7 days of *Pf* infection but recovered after drug treatment. This recovery may have been driven, at least in part, by increased levels of parasite molecules being available after drug-mediated killing to promote activation and/or expansion of certain immune cell subsets. Nevertheless, changes in these cell populations during malaria were transient, possibly reflecting the less persistent nature of *Plasmodium* infection, compared to HIV. Of note, we cannot exclude the possibility that reduced levels of circulating ILC1s, NK cells, and innate-like T cells following *Pf*

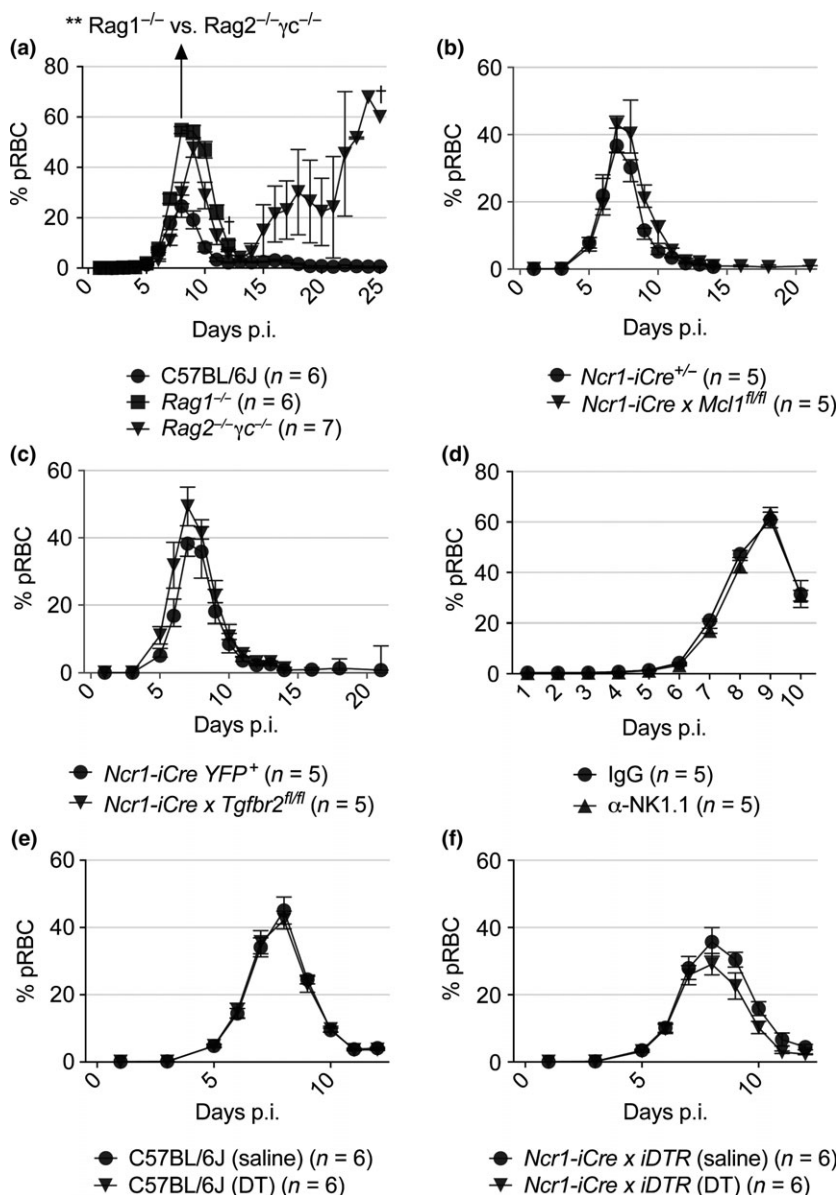


Figure 5. Depletion of cNK cells and ILC1s does not affect parasitaemia. C57BL/6J, Rag1^{-/-} and Rag2^{-/-}γc^{-/-} mice were infected with *PcAS*, and the kinetics of infection was measured (a). The kinetics of *PcAS* infection of *Ncr1-iCre* x *Mcl1*^{fl/fl} (b) and *Ncr1-iCre* x *Tgfbr2*^{fl/fl} (c) mice was compared to that of *Ncr1-iCre* and *Ncr1-iCre* YFP⁺ control mice, respectively. The kinetics of *PcAS* infection was also measured after administration of the monoclonal antibody (mAb) towards NK1.1 (α-NK1.1; clone: PK136) (d). Kinetics of parasitaemia in *Ncr1-iCre* x *iDTR* mice administered with diphtheria toxin is shown alongside the kinetics of parasitaemia for C57BL/6J control mice (e). Data in a represent results from three independent experiments with the peak parasitaemia of Rag1^{-/-}, and Rag2^{-/-}γc^{-/-} mice compared using the Mann–Whitney unpaired (nonparametric) *t*-test. Data in b, c, d represent results from one experiment. Error bars represent mean ± SEM. ***P* < 0.01.

infection or ILC1s following *PcAS* infection might reflect infection-mediated changes in the marker expression used to define our cell populations and/or sequestration of cells in tissues. This will require further examination.

We identified a cell population in the mouse liver that expressed both CD49a (an ILC1 marker)

and DX5 (a cNK cell marker). This population was also NK1.1- and NKp46-positive and expressed intermediate levels of TRAIL (expressed by ILC1s but not cNK cells) and CD62L (expressed by cNK cells but not ILC1s). These CD49a⁺ DX5⁺ double-positive cells emerged at 5 days p.i., which coincided with the loss of liver ILC1s. They were

also increased in frequency at 14 days p.i., when liver ILC1 frequency had yet to recover but were reduced at 28 days p.i., when the relative proportion of liver ILC1s to cNK cells resembled proportions prior to the loss of liver ILC1s. These cells were not liver-specific, as they were also found in the spleen. A recent report proposed a bidirectional plasticity between cNKs and ILC1s that was mediated by the presence or absence of Eomesodermin (Eomes).⁴⁵ Our current findings suggest that this CD49a⁺ DX5⁺ double-positive cell population may be an intermediate population between cNK cells and ILC1s. Recently, we reported a similar cell population expressing CD49a, CD49b and Eomes in mouse tumour models, and this was found to represent an intermediate population between TGF β -mediated conversion of cNK cells into ILC1s.⁴⁶ Whether this plasticity between cNKs and ILC1s also occurs in malaria remains unknown but perturbation of TGF β signalling following infection could help explain the disparity between ILC1 and NK cell frequencies after *PcAS* infection.

Although our results from mouse models of malaria indicate a limited role for cNK cells and ILC1s in control of parasite growth, we cannot exclude a role for these cells in human malaria, based on our data. Previous studies have shown that human NK cells rapidly produce IFN γ following exposure to *Pf* parasitised red blood cells (pRBCs) *in vitro*.^{29,47} Furthermore, depletion of NK cells in humanised mice infected with *Pf* using anti-CD56 mAb resulted in increased parasite growth,⁴⁸ albeit parasite growth appeared relatively modest in this model system. Nevertheless, our investigation of associations between cNK cells, ILC and innate-like T-cell subsets and either parasite burden (AUC) or PMR revealed no relationships. Further research is clearly needed in this area.

Our CHMI and mouse studies were initiated via an intravenous infusion of blood stage parasites, thereby bypassing the liver stage of infection. One advantage of this is that infections are relatively synchronous and hence, early changes in immune cell populations can be readily detected. However, it is possible that host responses to liver stage infections may influence subsequent responses to blood stage infections.⁴⁹ Recently, a study of innate-like T cells in CHMI studies in Tanzania using *Pf* sporozoites to establish infection reported changes in the frequencies of circulating NK and MAIT cells up to 6 months

after infection, although reduced frequencies of MAIT and NK cells were observed before this time point.³² The earliest samples were taken 9 days after infection in this study, making comparisons with our data difficult. Furthermore, the initiation of infection via liver stage, different parasite dose used to establish blood stage infection and the immune status of the Tanzanian volunteers living in a malaria-endemic region make direct comparisons with our data challenging. Nevertheless, comparisons between CHMI studies initiated with sporozoites and blood stage parasites in healthy volunteers and those living in malaria-endemic areas are likely to provide a wealth of future data that may help explain the roles of various immune cell populations during infection and disease, especially if infections initiated by liver and blood stages can be directly compared in the same populations.

In conclusion, we report a decline in the frequency of cNK cells, ILC1s, and innate-like T cells 7 days after blood stage *Pf* infection in CHMI studies with healthy volunteers. A similar observation was made for liver ILC1s in a mouse model of malaria caused by *PcAS*. Our data indicate a limited role for cNK cells and ILCs in the control of blood parasitaemia in mice. Together, these data provide novel insights into the responses of innate immune cells in mice and humans during malaria and may help guide future strategies aimed at manipulating host immune responses for clinical advantage during this disease.

METHODS

Controlled human malaria infection

Experimental procedures were performed as part of a substudy on human blood samples collected from consenting participants enrolled in a drug study (Australian New Zealand Clinical Trials Registry ACTRN12613000565741 and NCT02389348) conducted at Q-Pharm Pty Ltd (Herston, QLD, Australia) under the approval of the QIMR Berghofer Medical Research Institute Human Research Ethics Committee (QIMR-HREC). Volunteers comprised healthy male and female nonsmokers, aged between 18 and 45 in one trial and 18 and 55 in another trial, with no history of malaria or prior exposure to malaria-endemic regions. Experiments were performed on blood samples collected from participants enrolled in 3 cohorts ($n = 14$ volunteers in total). An additional cohort ($n = 8$ volunteers) was used to examine NK cell frequency and number. Participants were infected intravenously using a *Pf* (clone 3D7)-induced blood stage malaria (IBSM) challenge inoculum (1800 parasitised

red blood cells [pRBC]), with parasitaemia monitored by real-time quantitative polymerase chain reaction (qPCR),^{50–52} and blood collected at time points indicated in Results section. Antimalarial drug treatment was administered once parasitaemia exceeded 1000 parasites per mL.

Parasitaemia was plotted over time for each patient, and parasite burden over the course of infection (prior to treatment) was expressed as a measurement of AUC, as previously described.¹⁹ A growth model was also derived from parasitaemia measurements (prior to treatment) over time and fitted to each individual using simple linear regression. The gradient of this growth model (parasite multiplication rate [PMR]) was then estimated using a log-linear model described by the following equation:

$$\log_{10}(\Upsilon) = \alpha + m \times \text{time},$$

where Υ is parasites per mL measured by qPCR, α is the intercept, m is the gradient of the growth model, and time is the number of days from inoculation.

Isolation of peripheral blood mononuclear cells from human blood

Approximately 13 mL of blood was collected per volunteer, per time point, in BD Vacutainer® Lithium Heparin^N (LH) 170 I.U. Plus Blood Collection Tubes (BD Biosciences, San Jose, CA, USA). Blood was layered over Ficoll-Paque™ PLUS (GE Healthcare, Little Chalfont, Buckinghamshire, UK) to isolate peripheral blood mononuclear cells (PBMCs). PBMCs were counted using a hemocytometer.

Mice

Female mice between 8 and 12 weeks old were used. C57BL/6J (WT) mice were purchased from the Walter and Eliza Hall Institute (WEHI), Kew, VIC, Australia. *Rag1*^{-/-}, *Rag2*^{-/-}, *γc*^{-/-}, *Ncr1-iCre*, *Ncr1-iCre x iDTR*, *Ncr1-iCre YFP*⁺, *Ncr1-iCre x Mcl1*^{fl/fl} and *Ncr1-iCre x Tgfb2*^{fl/fl} mice all on the C57BL/6J genetic background were bred in house.^{42,53–61} All mice were housed under pathogen-free conditions at the QIMR Berghofer Medical Research Institute Animal Facility (Herston, QLD, Australia). Experimental use was in accordance with the 'Australian Code of Practice for the Care and Use of Animals for Scientific Purposes' (Australian National Health and Medical Research Council) and approved by the QIMR Berghofer Medical Research Institute Animal Ethics Committee (Herston, QLD, Australia; approval number: A02-633M).

PcAS infections and measurement of peripheral blood parasitaemia

PcAS was thawed from stabilities and passaged once *in vivo* in a C57BL/6J mouse, prior to establishing experimental infections. Mice were infected intravenously (i.v.) with 10⁵ pRBCs. Parasitaemia was measured by flow cytometry using Hoechst 33342 (Sigma-Aldrich®, St. Louis, MO, USA) and Syto 84 (Invitrogen™, Life Technologies, Carlsbad, CA, USA), as previously described.⁶² Samples were acquired on a BD FACSCanto™ II through BD FACSDiva™ V8.0 (both by BD

Biosciences) and analysed on FlowJo v10 OSX (Tree Star, Inc., Ashland, OR, USA).

Preparation of spleen and liver single-cell suspensions

Mice were sacrificed by CO₂ asphyxiation. A mid-sagittal incision was made on the abdominal cavity. The spleen was removed and passed through a 100-μm cell strainer (Corning Incorporated, Corning, NY, USA). The single-cell suspension was washed in Roswell Park Memorial Institute Medium (RPMI; Life Technologies) + 100 μg mL⁻¹ penicillin and streptomycin (ps; Gibco®, Life Technologies) (RPMI/ps) and incubated for 7 min in Red Blood Cell Lysis Buffer Hybri-Max™ (Sigma-Aldrich®). Cells were washed in RPMI/ps, pelleted by centrifugation and counted on the Countess II FL (Life Technologies), as per manufacturer's protocol. The liver was perfused with 1× phosphate-buffered saline (PBS). The excised liver was collected in 1% (v/v) foetal bovine serum (FBS) in PBS and mechanically passed through a 200-μm square metal mesh. Hepatocytes were separated from lymphocytes and removed using a 33% Percoll™ (GE Healthcare) gradient according to manufacturer's instructions. Red Blood Cell Lysis Buffer Hybri-Max™ was added to each pellet and incubated for 5 min at room temperature, prior to washing in 1% (v/v) FBS in PBS. Cells were pelleted by centrifugation and counted using the Countess II FL, as per manufacturer's protocol.

Identification of spleen and liver ILC1s using flow cytometry

Freshly prepared spleen and liver single-cell suspensions were incubated for 20 min with TruStain fcX™ (anti-mouse CD16/32; 93) and Zombie Aqua™ Fixable Viability Kit (both from BioLegend, San Diego, CA, USA) at room temperature. Cells were subsequently stained with a cell lineage cocktail containing biotin-conjugated anti-mouse CD3ε (145-2C11), CD5 (53–7.3) and CD19 (6D5) (all from BioLegend) at room temperature. Lineage-negative cells in splenocytes were concentrated by negative selection using the EasySep™ Biotin Positive Selection Kit (STEMCELL Technologies™, Vancouver, Canada) according to manufacturer's instructions. Surface staining included fluorophore-conjugated streptavidin (BioLegend) and fluorophore-conjugated anti-mouse monoclonal antibodies (mAb) against CD45 (30-F11), NK1.1 (PK136), NKp46 (29A1.4), CD49a (HMα1), CD49b (DX5), CD62L (MEL-14) (all from BioLegend) and TRAIL (CD253, N2B2) (eBioscience, San Diego, CA, USA).

Identification of human circulatory ILC1s in PBMCs

Freshly isolated PBMCs (2 × 10⁷) were incubated for 3 h with Phorbol 12-myristate 13-acetate (PMA) and ionomycin calcium salt (both from Sigma-Aldrich®) in complete media (RPMI/ps + 10% (v/v) FBS) with BD GolgiPlug™ Protein Transport Inhibitor and BD GolgiStop™ Protein Transport Inhibitor (containing Monensin) (both by BD Biosciences) at 37°C. PBMCs were then incubated with a cell lineage

cocktail containing fluorescein isothiocyanate (FITC)-conjugated mouse anti-human mAbs against CD123 (6H6), TCR α/β (IP26), TCR γ/δ (B1), CD14 (HCD14), CD34 (561), CD19 (HIB19) (BioLegend). PBMCs were incubated with a goat anti-mouse IgG biotinylated affinity-purified polyclonal antibody (R&D Systems™ by Bio-Techne, Minneapolis, Minnesota, USA). Lineage-negative (Lin⁻) cells were isolated using the EasySep™ Biotin Positive Selection Kit (STEMCELL Technologies™) according to manufacturer's instructions.

Lineage-negative cells were stained with a surface cocktail containing fluorophore-conjugated anti-human mAbs towards: CD56 (NCAM; HCD56), CD25 (BC96), Zombie Aqua™ Fixable Viability Kit, CD69 (FN50), and CD127 (A019D5) (all from BioLegend). Cells were then incubated with the Foxp3/Transcription Factor Staining Buffer Set (eBioscience) reagents according to manufacturer's instructions, followed by intracellular staining with an antibody cocktail containing fluorophore-conjugated anti-human mAbs against T-bet (4B10) (eBioscience) and IFN γ (4S.B3) (BioLegend).

Identification of human innate-like T cells in PBMCs

PBMCs (5×10^5) were incubated for 3 h with PMA and ionomycin calcium salt in complete media with BD GolgiPlug™ Protein Transport Inhibitor and BD GolgiStop™ Protein Transport Inhibitor (containing Monensin) at 37°C. PBMCs were stained with a surface cocktail containing fluorophore-conjugated anti-human mAbs against CD3 ϵ (UCHT1) (both from BD Pharmingen™, BD Biosciences), CD127 (A019D5), CD19 (HIB19) and CD56 (HCD56) (all from BioLegend) or a separate cocktail containing fluorophore-conjugated anti-human mAbs against CD161 (DX12) and CD3 ϵ (UCHT1) (both from BD Pharmingen™, BD Biosciences), CD4 (RPA-T4), CD8 α (SK1), Zombie Aqua™ Fixable Viability Kit, TCR V α 7.2 (3C10), TCR γ/δ (B1) (all from BioLegend) and human α -GalCer-loaded-CD1d PBS44 tetramer. In brief, sequences encoding human β 2M and the extracellular domain of human CD1d were cloned into the expression vector pHLsec and transfected into mammalian HEK-293S.GnTI cells.⁶³ Human β 2M encoding amino acid IQRTP to RDMGS and human CD1d encoding amino acid VPQRL to VLYWGS with a c-terminal BirA tag and His tag (amino sequence GLNDIFEAQKIEWHEHHHHHH) were purified using Nickel agarose purification and biotinylated using BirA enzyme. Biotinylated CD1d was loaded with PBS-44 provided by Paul Savage (Brigham Young University, Provo, UT) and converted to tetramers by the addition of streptavidin BV421 (eBioscience).

Cells were incubated with the Foxp3/Transcription Factor Staining Buffer Set (eBioscience) reagents according to manufacturer's instructions, followed by intracellular staining with an antibody cocktail containing fluorophore-conjugated anti-human mAbs towards PLZF (R17-809) and/or IFN γ (4S.B3) (both from BD Pharmingen™).

Flow cytometry

Samples were resuspended in 1% (w/v) paraformaldehyde (PFA) poststaining and stored at 4°C before acquisition on a

BD LSRFortessa™ (special order research product; BD Biosciences) through BD FACSDiva™ V8.0 and analysed on FlowJo v10 OSX.

Detection of apoptotic cells

Apoptotic cells were detected by cell surface staining with either Annexin V from the Annexin V FITC Apoptosis Detection Kit I (BD Biosciences) or reagents from the CellEvent® Caspase-3/7 Green Flow Cytometry Assay Kit (Molecular Probes®, Life Technologies), as per manufacturer's instructions.

Depletion of cNKs and ILC1s

C57BL/6J or *Rag1*^{-/-} mice were given an intraperitoneal (i.p.) injection with 1 mg per mouse of either anti-NK1.1 (PK136) mAb or *InVivo* MAb Polyclonal Mouse IgG (both from BioXCell, West Lebanon, New Hampshire, USA) on alternate days, starting from the day before infection.

Ncr1-iCre x iDTR mice were given 8 ng g⁻¹ (based on body weight) of DT from *Corynebacterium diphtheria* (Sigma-Aldrich®) per mouse 2 days and 1 day prior to infection and every 2 days after infection. Control mice were given an equal volume of sodium chloride (0.9% [w/v]) for irrigation (Baxter International, Deerfield, IL, USA). Depletion efficacy in both models was determined by flow cytometry analysis using an anti-mouse mAb towards NKp46 (CD335; 29A1.4) (BioLegend).

Statistics

Graphing and statistical analyses were performed on GraphPad Prism 6 (GraphPad, San Diego, CA, USA). A *P*-value (*P*) < 0.05 was considered statistically significant. Direct comparisons between two time points in the human trial data were made using the Wilcoxon (paired, nonparametric) test. For studies involving mice, comparisons between time points in time course experiments were made using the Kruskal–Wallis test accompanied by the Dunn's multiple comparisons test, while comparisons between two groups of mice were made using the Mann–Whitney (unpaired, nonparametric) *t*-test. All data are shown as mean \pm standard error of mean (SEM) unless otherwise stated.

ACKNOWLEDGMENTS

We thank the staff at Q-Pharm Pty. Ltd., Brisbane, Australia, for help in collecting blood samples and volunteers participating in clinical trials for allowing us to collect these samples. We thank Louise Marquart and Lachlan Webb for advice on statistics. Thanks to Joerg Moehrle and Tim Wells and Medicines for Malaria Venture (MMV) in Geneva for helpful discussions.

CONFLICT OF INTEREST

The authors declare no competing conflicts of interest.

REFERENCES

- Spits H, Artis D, Colonna M *et al.* Innate lymphoid cells—a proposal for uniform nomenclature. *Nat Rev Immunol* 2013; **13**: 145–149.
- Karo JM, Schatz DG, Sun JC. The RAG recombinase dictates functional heterogeneity and cellular fitness in natural killer cells. *Cell* 2014; **159**: 94–107.
- Yang Z, Tang T, Wei X *et al.* Type 1 innate lymphoid cells contribute to the pathogenesis of chronic hepatitis B. *Innate Immun* 2015; **21**: 665–673.
- Klose CS, Flach M, Mohle L *et al.* Differentiation of type 1 ILCs from a common progenitor to all helper-like innate lymphoid cell lineages. *Cell* 2014; **157**: 340–356.
- Vely F, Barlogis V, Vallentin B *et al.* Evidence of innate lymphoid cell redundancy in humans. *Nat Immunol* 2016; **17**: 1291–1299.
- Eberl G, Di Santo JP, Vivier E. The brave new world of innate lymphoid cells. *Nat Immunol* 2015; **16**: 1–5.
- Sojka DK, Plougastel-Douglas B, Yang L *et al.* Tissue-resident natural killer (NK) cells are cell lineages distinct from thymic and conventional splenic NK cells. *Elife* 2014; **3**: e01659.
- Doisne JM, Balmas E, Boulenouar S *et al.* Composition, development, and function of uterine innate lymphoid cells. *J Immunol* 2015; **195**: 3937–3945.
- Robinette ML, Fuchs A, Cortez VS *et al.* Transcriptional programs define molecular characteristics of innate lymphoid cell classes and subsets. *Nat Immunol* 2015; **16**: 306–317.
- Cortez VS, Cervantes-Barragan L, Robinette ML *et al.* Transforming growth factor-beta signaling guides the differentiation of innate lymphoid cells in salivary glands. *Immunity* 2016; **44**: 1127–1139.
- Victorino F, Sojka DK, Brodsky KS *et al.* Tissue-resident NK cells mediate ischemic kidney injury and are not depleted by anti-asialo-GM1 antibody. *J Immunol* 2015; **195**: 4973–4985.
- O'Sullivan TE, Rapp M, Fan X *et al.* Adipose-resident group 1 innate lymphoid cells promote obesity-associated insulin resistance. *Immunity* 2016; **45**: 428–441.
- Fuchs A, Vermi W, Lee JS *et al.* Intraepithelial type 1 innate lymphoid cells are a unique subset of IL-12- and IL-15-responsive IFN-gamma-producing cells. *Immunity* 2013; **38**: 769–781.
- Liehl P, Zuzarte-Luis V, Chan J *et al.* Host-cell sensors for Plasmodium activate innate immunity against liver-stage infection. *Nat Med* 2014; **20**: 47–53.
- Goncalves RM, Lima NF, Ferreira MU. Parasite virulence, co-infections and cytokine balance in malaria. *Pathog Glob Health* 2014; **108**: 173–178.
- Stephens R, Albano FR, Quin S *et al.* Malaria-specific transgenic CD4(+) T cells protect immunodeficient mice from lethal infection and demonstrate requirement for a protective threshold of antibody production for parasite clearance. *Blood* 2005; **106**: 1676–1684.
- Meding SJ, Cheng SC, Simon-Haarhaus B *et al.* Role of gamma interferon during infection with Plasmodium chabaudi chabaudi. *Infect Immun* 1990; **58**: 3671–3678.
- Walther M, Woodruff J, Edele F *et al.* Innate immune responses to human malaria: heterogeneous cytokine responses to blood-stage Plasmodium falciparum correlate with parasitological and clinical outcomes. *J Immunol* 2006; **177**: 5736–5745.
- Montes de Oca M, Kumar R, Rivera FL *et al.* Type I interferons regulate immune responses in humans with blood-stage Plasmodium falciparum infection. *Cell Rep* 2016; **17**: 399–412.
- Li C, Sanni LA, Omer F *et al.* Pathology of Plasmodium chabaudi chabaudi infection and mortality in interleukin-10-deficient mice are ameliorated by anti-tumor necrosis factor alpha and exacerbated by anti-transforming growth factor beta antibodies. *Infect Immun* 2003; **71**: 4850–4856.
- Lourembam SD, Sawian CE, Baruah S. Dysregulation of cytokines expression in complicated falciparum malaria with increased TGF-beta and IFN-gamma and decreased IL-2 and IL-12. *Cytokine* 2013; **64**: 503–508.
- Nasr A, Allam G, Hamid O *et al.* IFN-gamma and TNF associated with severe falciparum malaria infection in Saudi pregnant women. *Malar J* 2014; **13**: 314.
- Ho M, Sexton MM, Tongtawe P *et al.* Interleukin-10 inhibits tumor necrosis factor production but not antigen-specific lymphoproliferation in acute Plasmodium falciparum malaria. *J Infect Dis* 1995; **172**: 838–844.
- Ringwald P, Peyron F, Vuillez JP *et al.* Levels of cytokines in plasma during Plasmodium falciparum malaria attacks. *J Clin Microbiol* 1991; **29**: 2076–2078.
- Mohan K, Moulin P, Stevenson MM. Natural killer cell cytokine production, not cytotoxicity, contributes to resistance against blood-stage Plasmodium chabaudi AS infection. *J Immunol* 1997; **159**: 4990–4998.
- Yoshida O, Akbar F, Miyake T *et al.* Impaired dendritic cell functions because of depletion of natural killer cells disrupt antigen-specific immune responses in mice: restoration of adaptive immunity in natural killer-depleted mice by antigen-pulsed dendritic cell. *Clin Exp Immunol* 2008; **152**: 174–181.
- Nishikado H, Mukai K, Kawano Y *et al.* NK cell-depleting anti-asialo GM1 antibody exhibits a lethal off-target effect on basophils *in vivo*. *J Immunol* 2011; **186**: 5766–5771.
- Weidanz WP, LaFleur G, Brown A *et al.* Gammadelta T cells but not NK cells are essential for cell-mediated immunity against Plasmodium chabaudi malaria. *Infect Immun* 2010; **78**: 4331–4340.
- Artavanis-Tsakonas K, Eleme K, McQueen KL *et al.* Activation of a subset of human NK cells upon contact with Plasmodium falciparum-infected erythrocytes. *J Immunol* 2003; **171**: 5396–5405.
- Hansen DS, Siomos MA, Buckingham L *et al.* Regulation of murine cerebral malaria pathogenesis by CD1d-restricted NKT cells and the natural killer complex. *Immunity* 2003; **18**: 391–402.
- Hansen DS, Siomos MA, De Koning-Ward T *et al.* CD1d-restricted NKT cells contribute to malarial splenomegaly and enhance parasite-specific antibody responses. *Eur J Immunol* 2003; **33**: 2588–2598.
- Mpina M, Maurice NJ, Yajima M *et al.* Controlled human malaria infection leads to long-lasting changes in innate and innate-like lymphocyte populations. *J Immunol* 2017; **199**: 107–118.

33. Stephens R, Culleton RL, Lamb TJ. The contribution of *Plasmodium chabaudi* to our understanding of malaria. *Trends Parasitol* 2012; **28**: 73–82.
34. Korbel DS, Newman KC, Almeida CR et al. Heterogeneous human NK cell responses to *Plasmodium falciparum*-infected erythrocytes. *J Immunol* 2005; **175**: 7466–7473.
35. Horowitz A, Newman KC, Evans JH et al. Cross-talk between T cells and NK cells generates rapid effector responses to *Plasmodium falciparum*-infected erythrocytes. *J Immunol* 2010; **184**: 6043–6052.
36. Teirlinck AC, McCall MB, Roestenberg M et al. Longevity and composition of cellular immune responses following experimental *Plasmodium falciparum* malaria infection in humans. *PLoS Pathog* 2011; **7**: e1002389.
37. Engwerda CR, Minigo G, Amante FH et al. Experimentally induced blood stage malaria infection as a tool for clinical research. *Trends Parasitol* 2012; **28**: 515–521.
38. Spring M, Polhemus M, Ockenhouse C. Controlled human malaria infection. *J Infect Dis* 2014; **209**(Suppl 2): S40–S45.
39. Marquardt N, Beziat V, Nystrom S et al. Cutting edge: identification and characterization of human intrahepatic CD49a+ NK cells. *J Immunol* 2015; **194**: 2467–2471.
40. Engwerda CR, Beattie L, Amante FH. The importance of the spleen in malaria. *Trends Parasitol* 2005; **21**: 75–80.
41. White NJ. Malaria parasite clearance. *Malar J* 2017; **16**: 88.
42. Sathe P, Delconte RB, Souza-Fonseca-Guimaraes F et al. Innate immunodeficiency following genetic ablation of Mcl1 in natural killer cells. *Nat Commun* 2014; **5**: 4539.
43. Hviid L, Kurtzhals JA, Goka BQ et al. Rapid reemergence of T cells into peripheral circulation following treatment of severe and uncomplicated *Plasmodium falciparum* malaria. *Infect Immun* 1997; **65**: 4090–4093.
44. Klooverpris HN, Kazer SW, Mjosberg J et al. Innate lymphoid cells are depleted irreversibly during acute HIV-1 infection in the absence of viral suppression. *Immunity* 2016; **44**: 391–405.
45. Pikovskaya O, Chaix J, Rothman NJ et al. Cutting Edge: eomesodermin is sufficient to direct type 1 innate lymphocyte development into the conventional NK lineage. *J Immunol* 2016; **196**: 1449–1454.
46. Gao Y, Souza-Fonseca-Guimaraes F, Bald T et al. Tumor immunoevasion by the conversion of effector NK cells into type 1 innate lymphoid cells. *Nat Immunol* 2017; **18**: 1004–1015.
47. Artavanis-Tsakonas K, Riley EM. Innate immune response to malaria: rapid induction of IFN-gamma from human NK cells by live *Plasmodium falciparum*-infected erythrocytes. *J Immunol* 2002; **169**: 2956–2963.
48. Chen Q, Amaladoss A, Ye W et al. Human natural killer cells control *Plasmodium falciparum* infection by eliminating infected red blood cells. *Proc Natl Acad Sci U S A* 2014; **111**: 1479–1484.
49. Epiphany S, Mikolajczak SA, Goncalves LA et al. Heme oxygenase-1 is an anti-inflammatory host factor that promotes murine plasmodium liver infection. *Cell Host Microbe* 2008; **3**: 331–338.
50. McCarthy JS, Sekuloski S, Griffin PM et al. A pilot randomised trial of induced blood-stage *Plasmodium falciparum* infections in healthy volunteers for testing efficacy of new antimalarial drugs. *PLoS ONE* 2011; **6**: e21914.
51. McCarthy JS, Griffin PM, Sekuloski S et al. Experimentally induced blood-stage *Plasmodium vivax* infection in healthy volunteers. *J Infect Dis* 2013; **208**: 1688–1694.
52. Rockett RJ, Tozer SJ, Peatey C et al. A real-time, quantitative PCR method using hydrolysis probes for the monitoring of *Plasmodium falciparum* load in experimentally infected human volunteers. *Malar J* 2011; **10**: 48.
53. Mombaerts P, Iacomini J, Johnson RS et al. RAG-1-deficient mice have no mature B and T lymphocytes. *Cell* 1992; **68**: 869–877.
54. Shinkai Y, Rathbun G, Lam KP et al. RAG-2-deficient mice lack mature lymphocytes owing to inability to initiate V(D)J rearrangement. *Cell* 1992; **68**: 855–867.
55. Colucci F, Soudais C, Rosmaraki E et al. Dissecting NK cell development using a novel alymphoid mouse model: investigating the role of the c-abl proto-oncogene in murine NK cell differentiation. *J Immunol* 1999; **162**: 2761–2765.
56. Narni-Mancinelli E, Chaix J, Fenis A et al. Fate mapping analysis of lymphoid cells expressing the NKp46 cell surface receptor. *Proc Natl Acad Sci U S A* 2011; **108**: 18324–18329.
57. Vikstrom I, Carotta S, Luthje K et al. Mcl-1 is essential for germinal center formation and B cell memory. *Science* 2010; **330**: 1095–1099.
58. Glaser SP, Lee EF, Trounson E et al. Anti-apoptotic Mcl-1 is essential for the development and sustained growth of acute myeloid leukemia. *Genes Dev* 2012; **26**: 120–125.
59. Srinivas S, Watanabe T, Lin CS et al. Cre reporter strains produced by targeted insertion of EYFP and ECFP into the ROSA26 locus. *BMC Dev Biol* 2001; **1**: 4.
60. Buch T, Heppner FL, Tertilt C et al. A Cre-inducible diphtheria toxin receptor mediates cell lineage ablation after toxin administration. *Nat Methods* 2005; **2**: 419–426.
61. Chytil A, Magnuson MA, Wright CV et al. Conditional inactivation of the TGF-beta type II receptor using Cre: Lox. *Genesis* 2002; **32**: 73–75.
62. Edwards CL, Zhang V, Werder RB et al. Coinfection with blood-stage plasmodium promotes systemic type I interferon production during pneumovirus infection but impairs inflammation and viral control in the lung. *Clin Vaccine Immunol* 2015; **22**: 477–483.
63. Aricescu AR, Lu W, Jones EY. A time- and cost-efficient system for high-level protein production in mammalian cells. *Acta Crystallogr D Biol Crystallogr* 2006; **62**: 1243–1250.

Supporting Information

Additional Supporting Information may be found online in the supporting information tab for this article.



This is an open access article under the terms of the Creative Commons Attribution License, which permits use, distribution and reproduction in any medium, provided the original work is properly cited.